

^{17}O ENDOR Detection of a Solvent-Derived Ni–(OH_x)–Fe Bridge That Is Lost upon Activation of the Hydrogenase from *Desulfovibrio gigas*

Marta Carepo,[†] David L. Tierney,^{‡,§} Carlos D. Brondino,^{†,‡} Tran Chin Yang,[‡]
Ana Pamplona,[†] Joshua Telser,^{‡,||} Isabel Moura,[†] José J. G. Moura,^{*,†} and
Brian M. Hoffman^{*,‡}

Contribution from the Departamento de Química and Centro de Química Fina e Biotecnologia, Faculdade de Ciências e Tecnologia, Universidade Nova de Lisboa, 2825-114 Monte de Caparica, Portugal, and Department of Chemistry, Northwestern University, Evanston, Illinois 60208-3113

Received January 24, 2001

Abstract: Crystallographic studies of the hydrogenases (Hases) from *Desulfovibrio gigas* (*Dg*) and *Desulfovibrio vulgaris* Miyazaki (*DvM*) have revealed heterodinuclear nickel–iron active centers in both enzymes. The structures, which represent the as-isolated (unready) Ni-A ($S = 1/2$) enzyme state, disclose a nonprotein ligand (labeled as X) bridging the two metals. The bridging atom was suggested to be an oxygenic (O^{2-} or OH^-) species in *Dg* Hase and an inorganic sulfide in *DvM* Hase. To determine the nature and chemical characteristics of the Ni–X–Fe bridging ligand in *Dg* Hase, we have performed 35 GHz CW ^{17}O ENDOR measurements on the Ni-A form of the enzyme, exchanged into H_2^{17}O , on the active Ni-C ($S = 1/2$) form prepared by H_2 -reduction of Ni-A in H_2^{17}O , and also on Ni-A formed by reoxidation of Ni-C in H_2^{17}O . In the native state of the protein (Ni-A), the bridging ligand does not exchange with the H_2^{17}O solvent. However, after a reduction/reoxidation cycle (Ni-A \rightarrow Ni-C \rightarrow Ni-A), an ^{17}O label is introduced at the active site, as seen by ENDOR. Detailed analysis of a 2-D field-frequency plot of ENDOR spectra taken across the EPR envelope of Ni-A(^{17}O) shows that the incorporated ^{17}O has a roughly axial hyperfine tensor, $\mathbf{A}(^{17}\text{O}) \approx [5, 7, 20]$ MHz, discloses its orientation relative to the \mathbf{g} tensor, and also yields an estimate of the quadrupole tensor. The substantial isotropic component ($a_{\text{iso}}(^{17}\text{O}) \approx 11$ MHz) of the hyperfine interaction indicates that a solvent-derived ^{17}O is indeed a ligand to Ni and thus that the bridging ligand X in the Ni-A state of *Dg* Hase is indeed an oxygenic (O^{2-} or OH^-) species; comparison with earlier EPR results by others indicates that the same holds for Ni-B. The small ^{57}Fe hyperfine coupling seen previously for Ni-A ($A(^{57}\text{Fe}) \sim 0.9$ MHz) is now shown to persist in Ni-C, $A(^{57}\text{Fe}) \sim 0.8$ MHz. However, the ^{17}O signal is lost upon reductive activation to the Ni-C state; reoxidation to Ni-A leads to the reappearance of the signal. Consideration of the electronic structure of the EPR-active states of the dinuclear center leads us to suggest that the oxygenic bridge in Ni-A(B) is lost in Ni-C and is re-formed from solvent upon reoxidation to Ni-A. This implies that the reductive activation to Ni-C opens Ni/Fe coordination sites which may play a central role in the enzyme's activity.

Hydrogenases (Hases) catalyze the reversible oxidation of molecular hydrogen according to the reaction $\text{H}_2 \leftrightarrow 2\text{H}^+ + 2\text{e}^-$. The native hydrogenase from *Desulfovibrio gigas* (*Dg*), purified under aerobic conditions, gives two types of EPR signals from inactive enzyme forms: a major signal referred to as Ni-A with $g_{1,2,3} = [2.31, 2.23, 2.01]$ and a minor one, Ni-B, with $g_{1,2,3} =$

$[2.33, 2.16, 2.01]$.^{1–3} The Ni-A state is called the “unready” state of the enzyme as activation requires prolonged exposure to hydrogen, whereas Ni-B, known as the “ready” state, can be rapidly activated. Reduction of the Ni-A state with hydrogen gas generates an active form of the enzyme, termed Ni-C, which is EPR-active with $g_{1,2,3} = [2.19, 2.14, 2.01]$. Two EPR-silent states also are observed in this enzyme, Ni-SI and N-R, the first corresponding to an intermediate state between Ni-A/B and Ni-C and the second corresponding to the fully reduced protein.^{4,5}

* To whom correspondence should be addressed. B.M.H.: Tel., +1-847-4913104; Fax, +1-847-4917713; E-mail, bmh@northwestern.edu. J.J.G.M.: Tel., +351-21-2948382; Fax, +351-21-2948550; E-mail, jose.moura@dq.fct.unl.pt.

[†] Universidade Nova de Lisboa.

[‡] Northwestern University.

[§] Present address: Department of Chemistry, University of New Mexico, Albuquerque, NM 87131.

^{||} C.D.B. is also at Facultad de Bioquímica y Cs. Biológicas, UNL, Santa Fe, Argentina.

^{||} Permanent address: Chemistry Program, Roosevelt University, Chicago, IL 60605.

(1) Albracht, S. P. J.; Kalkman, M. L.; Slater, E. C. *Biochim. Biophys. Acta* **1983**, *724*, 309–316.

(2) LeGall, J.; Ljungdahl, P. O.; Moura, I.; Peck, H. D., Jr.; Xavier, A. V.; Moura, J. J. G.; Teixeira, M.; Huynh, B. H.; DerVartanian, D. V. *Biochem. Biophys. Res. Commun.* **1982**, *106*, 610–616.

(3) Fernandez, V. M.; Hatchikian, E. C.; Cammack, R. *Biochim. Biophys. Acta* **1985**, *832*, 69–79.

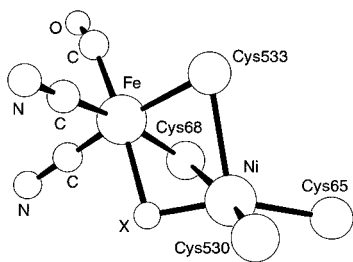


Figure 1. Active site structure of the *Dg* [Ni-Fe] hydrogenase.⁷

Crystallographic studies of the *Dg* [NiFe] Hase^{6,7} in the native state at 2.85 and 2.54 Å resolution revealed a heterodinuclear nickel-iron active center. Four cysteine thiolates coordinate the Ni atom, two as terminal ligands and two bridging the Ni and Fe atoms (Figure 1). The Fe atom was identified as a diamagnetic low-spin Fe(II) in a previous ⁵⁷Fe pulsed ENDOR study of *Dg* Hase.⁸ The iron is coordinated by three exogenous diatomic ligands, identified by the combination of X-ray crystallography and FTIR measurements as two CN⁻ and one CO.⁹ The iron ligands differ slightly for the [NiFe] hydrogenase from *Desulfovibrio vulgaris* Miyazaki (*DvM*), where the crystal structure (1.8 Å resolution) has identified one SO, one CO, and one CN⁻ bound to Fe.¹⁰

In the electron density map of the 2.54 Å structure of *Dg* Hase,^{6,7} an additional small peak was observed at a bridging position between the two metal ions. The nature of this bridging ligand, represented in Figure 1 as X, could not be determined, but was suggested to be an oxygenic species. Prior EPR evidence for the interaction of ¹⁷O with the dinuclear center was reported for *Chromatium vinosum* (*Chv*) Hase,¹¹ although the authors concluded from the small value of the coupling constant (derived from EPR line broadening) that oxygen was not a ligand to the nickel. In the native *DvM* Hase structure, a bridging ligand also is present, but this was assigned as an inorganic sulfide. X-ray structures of the reduced *DvM* and [NiFeSe] *Desulfomicrobium baculatus* hydrogenases showed that the bridging ligand is not present in this state.^{12,13}

In this work we address the nature and the lability of the bridging ligand in *Dg* Hase in the Ni-A and Ni-C states by ¹⁷O ENDOR spectroscopy on the unready Ni-A enzyme form exchanged into H₂¹⁷O, on the active Ni-C form prepared by H₂-reduction of Ni-A in H₂¹⁷O, and on Ni-A prepared by reoxidation of Ni-C in H₂¹⁷O, repeating this cycle several times. As the first H₂¹⁷O ENDOR study performed on hydrogenase, the results provide direct evidence for the presence of a solvent-derived oxygenic species as the bridging ligand in the native enzyme and suggest that it is lost upon activation to Ni-C.

Materials and Methods

Protein Purification. *D. gigas* (NCIMB 9332) hydrogenase (⁵⁷Fe-enriched and natural abundance samples) was purified according to published procedures.^{14,15} The purity of the protein was followed by the ratio of A₄₀₀ to A₂₈₀, with a final value of 0.26. SDS-polyacrylamide electrophoresis was used to establish the protein purity.

Preparation of Samples for Q-Band ENDOR Spectroscopy. Purified hydrogenases were concentrated in a centricon (Amicon YM30) to approximately 1 mM in Tris/HCl buffer (100 mM, pH 7.6). The native protein (natural abundance) was exchanged in a centricon with H₂¹⁷O (50.7% ¹⁷O) purchased from MSD ISOTOPIES (Division of Merck Frost Canada Inc., Montreal) to a final enrichment of ~40%. The protein was then transferred with a syringe fitted with Teflon tubing to a Q-band ENDOR tube. EPR spectra of the starting Ni-A enzyme (not shown) displayed <5% of the minority Ni-B state. The Ni-C state was generated by exposing samples to H₂ gas and by monitoring changes in the Ni EPR signal. Ni-C samples were reoxidized by exposure to air and again by monitoring the Ni EPR. The ⁵⁷Fe Hase ENDOR sample was reduced to Ni-C as described above.

ENDOR Spectroscopy. ENDOR spectra were collected on Q-band CW¹⁶ and pulsed¹⁷ spectrometers described previously. In collecting ¹⁷O ENDOR signals, we employed noise broadening of the rf to enhance sensitivity,¹⁸ and it was also important to use a low-pass (~30 MHz) filter to remove rf harmonics that excited the proton ENDOR response. The ENDOR spectra for ¹⁷O (*I* = 5/2) reported here consist of the ν₊ branch of the spectrum, where a single-crystal-like spectrum consists of two branches, ν_±(¹⁷O) = ν₀ ± A(¹⁷O)/2 (each branch is further split, when resolved, by the quadrupole interaction); here ν₀ is the ¹⁷O Larmor frequency, and A(¹⁷O) is the hyperfine coupling. For ⁵⁷Fe (*I* = 1/2), two peaks, at ν_±(⁵⁷Fe) = ν₀ ± A(⁵⁷Fe)/2, are expected. Analysis procedures have been described for deriving spin-Hamiltonian parameters from a 2-D set of orientation-selective spectra, taken from a frozen solution, at multiple fields across the EPR envelope.^{19–21} The simulations of these 2-D patterns were performed both with program GENDOR,^{20,21} which employs first-order equations for both hyperfine and quadrupole interactions, and with DDPOWHE, which employs exact solutions of the nuclear energies for arbitrary ¹⁷O hyperfine and quadrupole tensors²² (both available on the Web, <http://www.gendor1.chem.northwestern.edu>).

Results

The ENDOR spectrum collected in the ~7–20 MHz range at the low-field edge of the EPR signal (*g*₁ = 2.31) of the Ni-A enzyme exchanged into H₂¹⁷O solvent is featureless, as is that of the Ni-A enzyme in H₂¹⁶O (Figure 2A).²³ The absence of a signal that can be attributed to ¹⁷O indicates either that the

- (4) Roberts, L. M.; Lindahl, P. A. *Biochemistry* **1994**, *33*, 14339–14350.
- (5) Roberts, L. M.; Lindahl, P. A. *J. Am. Chem. Soc.* **1995**, *117*, 2565–2572.
- (6) Volbeda, A.; Charon, M.-H.; Piras, C.; Hatchikian, E. C.; Frey, M.; Fontecilla-Camps, J. C. *Nature* **1995**, *373*, 580–587.
- (7) Volbeda, A.; Garcin, E.; Piras, C.; de Lacey, A. L.; Fernandez, V. M.; Hatchikian, E. C.; Frey, M.; Fontecilla-Camps, J. C. *J. Am. Chem. Soc.* **1996**, *118*, 12989–12996.
- (8) Huyett, J. E.; Carepo, M.; Pamplona, A.; Franco, R.; Moura, I.; Moura, J. J. G.; Hoffman, B. M. *J. Am. Chem. Soc.* **1997**, *119*, 9291–9292.
- (9) Happe, R.; Rosenboom, W.; Pierik, A. J.; Albracht, S. P. J.; Bagley, K. A. *Nature (London)* **1997**, *385*, 126.
- (10) Higuchi, Y.; Yagi, T.; Yasuoka, N. *Structure* **1997**, *5*, 1671–1680.
- (11) van der Zwaan, J. W.; Coremans, J. M. C. C.; Bouwens, E. C. M.; Albracht, S. P. J. *Biochim. Biophys. Acta* **1990**, *1041*, 101–110.
- (12) Higuchi, Y.; Ogata, H.; Miki, K.; Yasuoka, N.; Yagi, T. *Structure* **1999**, *7*, 549–556.
- (13) Garcin, E.; Vernede, X.; Hatchikian, E. C.; Volbeda, A.; Frey, M.; Fontecilla-Camps, J. C. *Structure* **1999**, *7*, 557–566.

- (14) Teixeira, M.; Moura, I.; Xavier, A. V.; Moura, J. J. G.; LeGall, J.; DerVartanian, D. V.; Peck, J.; Harry, D.; Huynh, B.-H. *J. Biol. Chem.* **1989**, *264*, 16435–16450.
- (15) Teixeira, M.; Moura, I.; Xavier, A. V.; Huynh Boi, H.; DerVartanian, D. V.; Peck, H. D., Jr.; LeGall, J.; Moura, J. J. G. *J. Biol. Chem.* **1985**, *260*, 8942–8950.
- (16) Werst, M. M.; Davoust, C. E.; Hoffman, B. M. *J. Am. Chem. Soc.* **1991**, *113*, 1533–1538.
- (17) Davoust, C. E.; Doan, P. E.; Hoffman, B. M. *J. Magn. Reson.* **1996**, *119*, 38–44.
- (18) Hoffman, B. M.; DeRose, V. J.; Ong, J. L.; Davoust, C. E. *J. Magn. Reson.* **1994**, *110*, 52–57.
- (19) Hoffman, B. M.; Martinsen, J.; Venters, R. A. *J. Magn. Reson.* **1984**, *59*, 110–123.
- (20) Hoffman, B. M.; DeRose, V. J.; Doan, P. E.; Gurbel, R. J.; Houseman, A. L. P.; Telser, J. In *Biological Magnetic Resonance*; Berliner, L. J., Reuben, J., Eds.; Plenum Press: New York and London, 1993; Vol. 13, pp 151–218.
- (21) DeRose, V. J.; Hoffman, B. M. *Methods Enzymol.* **1995**, *246*, 554–589.
- (22) Telser, J.; Horng, Y.-C.; Becker, D. F.; Hoffman, B. M.; Ragsdale, S. W. *J. Am. Chem. Soc.* **2000**, *122*, 182–183.
- (23) Features seen near ~4–6 MHz in both the presence and the absence of labeled dioxygen will be ignored.

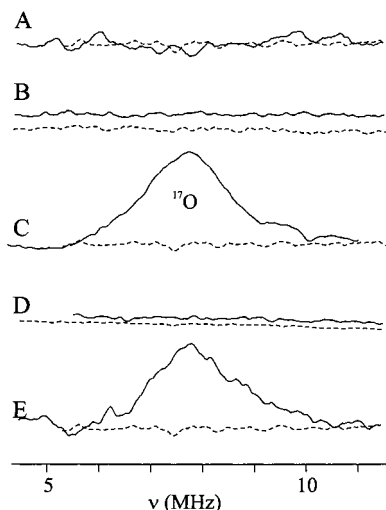


Figure 2. A 35 GHz CW ENDOR of Dg Hase in H₂¹⁶O (dashed) and in H₂¹⁷O (solid). (A) Ni-A, exchanged into H₂¹⁷O. (B) Ni-C in H₂¹⁷O, generated by H₂-reduction of the Ni-A samples from 2A. (C) Ni-A in H₂¹⁷O after one reduction/reoxidation cycle, (Ni-A → Ni-C → Ni-A). (D) Ni-C, generated by H₂-reduction of the Ni-A samples from 2C. (E) Ni-A in H₂¹⁷O after two reduction/reoxidation cycles, (Ni-A → Ni-C → Ni-A → Ni-C → Ni-A). Conditions: $g_1 = 2.31$ (Ni-A) or 2.19 (Ni-C); $T = 2$ K; $\nu_{\text{MW}} = 35.0$ GHz; MW power = 400 μ W; 8 G field modulation (100 kHz); time constant = 32 ms; RF power = 25 W (100 kHz bandwidth broadened); 3 MHz s⁻¹ scan rate; receiver gain = 1000; 20 scans.

bridging ligand is not an oxygenic species or that this species is not exchangeable with solvent; the latter possibility was suggested by previous ¹H and ²H ENDOR studies which indicated the Ni-A state to be inaccessible to H/D exchange.²⁴ The Ni-A sample in H₂¹⁷O solvent was then H₂-reduced to the Ni-C state. ENDOR measurements on this Ni-C sample (Figure 2B) also show no signals that can be associated with ¹⁷O.

The Ni-C sample in H₂¹⁷O was then reoxidized to Ni-A, corresponding to one reduction/reoxidation cycle in H₂¹⁷O solvent: Ni-A → Ni-C → Ni-A. ENDOR measurements performed on the resulting Ni-A ($g_1 = 2.31$; Figure 2C) showed an intense signal at 8.5 MHz that is not present for the similar sample in H₂¹⁶O and must therefore arise from ¹⁷O. Taking this feature as $\nu_+(\text{¹⁷O}) = (\nu(\text{¹⁷O}) + A(\text{¹⁷O}))/2$, where $\nu(\text{¹⁷O}) = 6.25$ MHz, yields $A_1(\text{¹⁷O}) \approx 5$ MHz; the breadth of the $\nu_+(\text{¹⁷O})$ line likely is determined by an unresolved ¹⁷O ($I = 5/2$) quadrupole interaction as seen in other ¹⁷O ENDOR studies,²⁵ in which case it corresponds roughly to 12 times the quadrupole coupling, suggesting $|P_1| \approx 0.1\text{--}0.2$ MHz. This signal was also observed for the Ni-A states generated during subsequent reduction/reoxidation cycles, while no ¹⁷O signals were observed for the Ni-C states generated during any of these cycles (Figure 2D and E).

In a previous ¹⁷O EPR study of Chv Hase,¹¹ samples in the Ni-C state were reoxidized with ¹⁷O₂ gas to the Ni-A/Ni-B state. Although no resolved ¹⁷O hyperfine was observed, all three canonical features of the EPR spectrum for Ni-A and the g_2 and g_3 features for Ni-B showed ¹⁷O broadening, suggesting a weak interaction between the Ni and oxygen atoms. These observations were interpreted as an oxygen atom/molecule in the vicinity of Ni but not directly coordinated to the metal. To

address this issue, a set of orientation-selective ENDOR spectra of the $\nu_+(\text{¹⁷O})$ features was collected over most of the EPR envelope of the Ni-A ¹⁷O sample used to obtain Figure 2E (see Materials and Methods). As seen in Figure 3A, data could be collected from $g_1 = 2.31$ to $g \approx 2.03$; only fields from $g \approx 2.03$ to $g_3 = 2.01$ were inaccessible due to an overlap with the EPR signal of the Hase Fe-S cluster.

As we now discuss, the 2-D field-frequency plot of $\nu_+(\text{¹⁷O})$ ENDOR features in Figure 3A displays the pattern of a near-axial hyperfine tensor which is rotated relative to the **g** tensor by an angle θ about the common (g_1, A_1) axis, with the unique (largest) component, A_3 , lying in the $g_2\text{--}g_3$ plane.¹⁹ As noted above, the signals show no resolved splitting by the quadrupole interaction; differential broadening of various features can be attributed to unresolved quadrupole couplings, as described recently for the two ¹⁷O atoms incorporated in the diiron center of intermediate X of *E. coli* ribonucleotide reductase.²⁵ The 2-D field-frequency pattern is determined by the anisotropic ¹⁷O hyperfine interaction. The spectrum at g_1 is a single-crystal-like ν_+ peak arising from those molecules in the frozen solution where the external field lies along the (g_1, A_1) axis, and thus the hyperfine coupling at this field is $A_1(\text{¹⁷O}) \approx 5$ MHz. As the field is increased (g decreases), this feature splits into two branches. The lower-frequency (“1–3”) branch,^{19,26} which connects the single-crystal-like spectra that appear at g_1 and at g_3 , shifts little with the field until the field begins to approach g_3 . The frequency (hyperfine coupling) of the other (“1–2”) branch increases rapidly until the field reaches $g_2 = 2.23$ where this branch appears as an intense peak at $\nu \approx 15$ MHz, corresponding to the signal from those centers where the field lies along g_2 . As the field is increased further, this peak quickly splits into two subbranches which together form the “2–3” branch. These diverge until $g \approx 2.11$, at which point the maximum-frequency peak in the 2-D pattern is observed; this peak corresponds to the largest principal hyperfine component and gives $A_3(\text{¹⁷O}) \approx 19\text{--}20$ MHz. This peak also is the broadest in the pattern, indicating that the largest quadrupole tensor component lies roughly parallel to A_3 ; the breadth suggests that its value is $P_{11} \approx 0.2\text{--}0.3$ MHz. As g is further decreased, the subbranches converge and would coalesce with the “1–3” branch at the single-crystal-like position of $g_3 = 2.01$ if that field could be accessed.

It is the splitting of the “2–3” branch and the absence of splitting of the other branches which indicate that $A_1(\text{¹⁷O})$ lies along g_1 and that the hyperfine tensor is rotated about g_1 . Following established procedures,^{19–21} the occurrence of the largest hyperfine splitting at $g \approx 2.11$ not only yields $A_3(\text{¹⁷O})$, given above, but also defines the angle of rotation to be $\theta \approx 45^\circ$. Although no single spectrum has a peak that directly gives $A_2(\text{¹⁷O})$, this value can be calculated from the coupling associated with the intense peak at g_2 , through use of the values for $A_3(\text{¹⁷O})$ and θ : $A_2(\text{¹⁷O}) \approx 7$ MHz.

Because of the relatively limited number of complete studies of powder ¹⁷O ENDOR (see ref 25), this analysis has been tested through simulations using both exact solutions of the nuclear energies for arbitrary ¹⁷O hyperfine and quadrupole tensors, as

(24) Fan, C.; Teixeira, M.; Moura, J.; Moura, I.; Huynh, B.-H.; le Gall, J.; Peck, H. D., Jr.; Hoffman, B. M. *J. Am. Chem. Soc.* **1991**, *113*, 20–24.
 (25) Burdi, D.; Willems, J.; Riggs-Gelasco, P.; Antholine, W.; Stubbe, J.; Hoffman, B. *J. Am. Chem. Soc.* **1998**, *120*, 12910–12919.

(26) Regardless of the relative orientation of the **A** and **g** tensors, there is a well-defined hyperfine coupling whenever the external field lies along each of the three **g** axes. The “*i*-*j*” branch connects two such couplings at their corresponding **g** values.

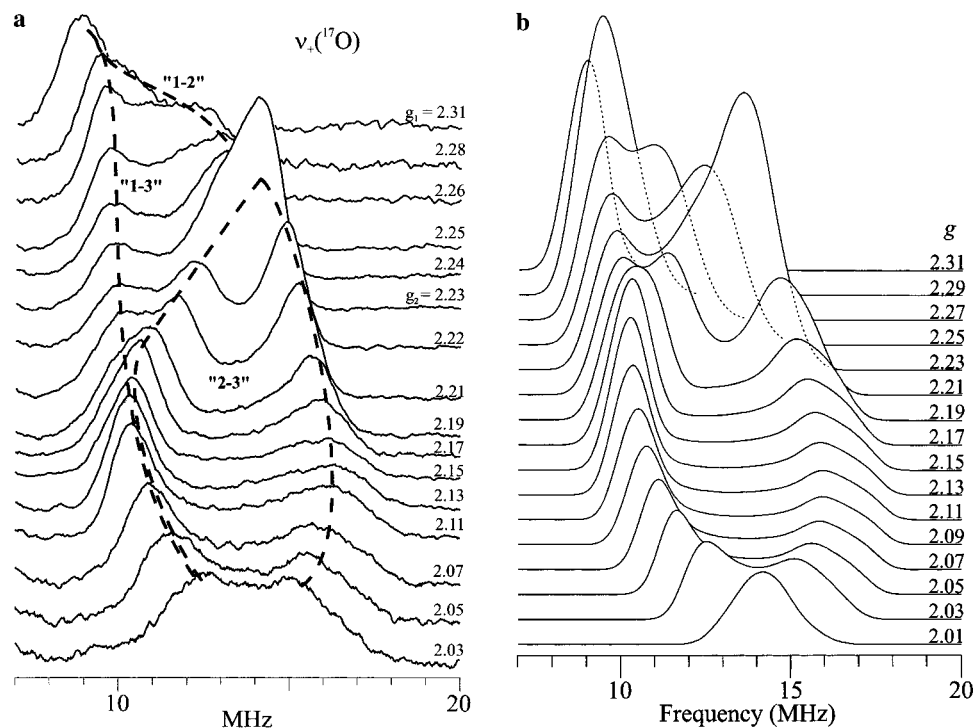


Figure 3. (A) A 2-D field-frequency plot of 35 GHz CW ENDOR spectra of Ni-A D_g Hase after redox cycling in $H_2^{17}O$ (Ni-A \rightarrow Ni-C \rightarrow Ni-A). For clarity in presentation this is a partial set, with an additional number of spectra having been deleted; the symbols “ i, j ” label the “branches” discussed in the text. Conditions: Observing g -value as indicated on the plot. All other conditions as in Figure 2. Dashed line is to guide the eye (see text). (B) Simulations of the 2-D pattern by program GENDOR. Parameters: $\mathbf{A} = [7, 5, 20]$ MHz, $\phi = 90$, $\theta = 45$ (the permutation of the first two values arises from the definition of Euler angles employed); $\mathbf{P} = [-0.075, -0.075, 0.15]$ MHz and is coaxial with \mathbf{A} ; ENDOR line width, 0.5 MHz, EPR line width, 70 MHz.

done previously,²⁵ and the first-order treatment.^{20,21} In both approaches, calculations that employ the ^{17}O hyperfine tensor and quadrupole tensor with maximum value $P_{||}$, as discussed above, with no significant adjustment, fully reproduce not only the overall 2-D pattern of Figure 3A, but also the details of the individual spectra, as shown in Figure 3B. The results of the two approaches are the same except for slight variations in the shapes of the rather poorly defined high-frequency “2–3” subbranch feature and resulting slight differences (<0.1 MHz) in $P_{||}$.²⁷ We thus more or less arbitrarily chose the first-order calculation to present in Figure 3B, which employed $\mathbf{A} = [5, 7, 20]$ MHz, isotropic component, $a_{iso}(^{17}O) = 11$ MHz.²⁸ Simulations in which the input parameters were varied indicated that the hyperfine tensor components are specified to within $\lesssim \pm 1$ MHz; uncertainties of the rotation angle $\theta = 45^\circ$ are small, $\lesssim 5^\circ$; the direction of the unique hyperfine tensor component may lie out of the g_2 – g_3 plane (deviation of the Euler angle ϕ from 90°) by as much as ca. 15° .

In light of the loss of the oxygen-bridge ^{17}O signal for Ni-C, we reexamined the Ni–Fe interaction in this state. In our previous 35 GHz pulsed ENDOR study of ^{57}Fe enriched D_g Hase,⁸ the Ni(III) center in the Ni-A state was shown to have a hyperfine coupling of $A_2 \approx 1$ MHz to a diamagnetic, low-spin $^{57}Fe(II)$, but no ^{57}Fe signal was seen for the Ni-C state. Upon reexamining ^{57}Fe D_g Hase in the Ni-C state with 35 GHz Mims pulsed ENDOR at $g_2 = 2.14$, we obtained a spectrum (Figure 4) with a weak ^{57}Fe doublet centered at $\nu(^{57}Fe)$. The hyperfine splitting of $A_2 \approx 0.8$ MHz is comparable to that

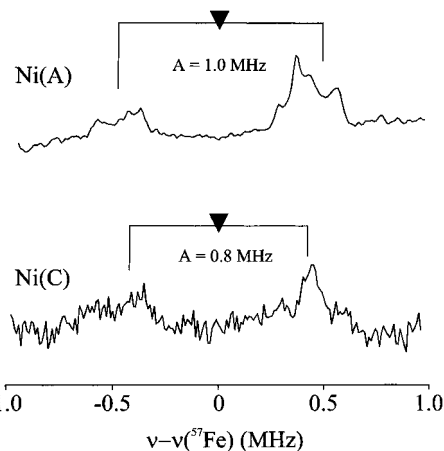


Figure 4. A 35 GHz Mims pulsed ^{57}Fe ENDOR of Ni-A ($g_2 = 2.23$) and Ni-C ($g_2 = 2.14$) D_g Hase. Conditions: $T = 2$ K, $\nu_{MW} = 34.7$ GHz, MW pulse lengths = 48 ns, $\tau = 452$ ns, RF pulse length = 40 μ s, repetition rate = 25 Hz. The spectrum consists of 256 points, with each point an average of 400 transients.

observed previously for Ni-A. The coupling in both states must arise primarily from a small amount of spin density delocalized onto the Fe(II), rather than from a through-space dipolar interaction with spin on Ni. At the crystallographically determined Ni–Fe distance of $\lesssim 3$ Å,^{6,7} the dipolar interaction between an electron spin located primarily on Ni and the ^{57}Fe nucleus is at most ~ 0.2 MHz, a small fraction of the measured coupling.

Discussion

The nickel ion in the dinuclear Ni/Fe center of D_g Hase exhibits a distorted square-pyramidal geometry, with the sulfur

(27) This likely represents different handling of the line widths and of the integration algorithms and does not detract from the identity of the simulations in all essential elements.

(28) The full set of simulation parameters is given in the figure legend.

of Cys 533 at the apex; three other cysteinyl sulfurs plus the bridge, X, form a highly distorted square, Figure 1.^{6,7} The present ENDOR experiments show that the Ni-A form of this center of *Dg* Hase exhibits an ¹⁷O signal from a solvent-derived species. The signal disappears upon redox cycling to Ni-C and reappears upon reoxidation to the Ni-A state. The ¹⁷O hyperfine tensor, with principal values $\mathbf{A}({}^{17}\text{O}) = [5, 7, 20]$ MHz, has a substantial isotropic component ($a_{\text{iso}}({}^{17}\text{O}) \approx 11$ MHz), indicating the presence of a Ni–O bond. This establishes that a solvent-derived ¹⁷O is indeed coordinated to the Ni in Ni-A, X in Figure 1. The observation by van der Zwaan et al.¹¹ of ¹⁷O broadening for both ¹⁷O₂-oxidized Ni-A and Ni-B then indicates that Ni-B also contains a solvent-derived bridge. The exact nature of the bridge in Ni-A (μ -oxo, μ -hydroxo, or μ -aquo) remains to be determined. EXAFS studies of *Dg* and *Chv* Hases did not show a short Ni–O distance in the Ni-A state, which was interpreted as evidence against a μ -oxo bridge, the distances observed (1.91 Å for *Cv*) being more consistent with a hydroxy bridge.^{29,30}

There are two possible explanations for the loss of the ¹⁷O signal in Ni-C: loss of the bridge itself or loss of the ¹⁷O ENDOR signal because the hyperfine coupling in Ni-C is reduced to the point that it is comparable to the ¹⁷O quadrupole coupling, which might weaken and broaden the ENDOR signal into undetectability. We consider this latter possibility in the context of current understanding of the electronic structures of the Ni-A,B and Ni-C dinuclear centers, as summarized in the elegant single-crystal EPR study by Trofanchuk et al. of the NiFe Hase from *Dv* Miyazaki F, whose *g* values are essentially the same as those of the *Dg* Hase.³¹

The pattern of *g* values exhibited by the Ni-A,B,C centers ($g_1 \sim g_2 > g_3 \sim g_e$) shows that in each of the three states the odd electron is on a Ni(III) ion in a 3d_{z²} orbital, with the *g*₃ tensor axis lying along the axis of that orbital (*z*). As a result, we can discuss the ¹⁷O signal that is observed for *Dg* Hase Ni-A and that is lost for Ni-C, in light of the extensive body of information about hyperfine couplings to ligands in square-pyramidal Ni(III) and Co(II) complexes with a d_{z²} configuration. In such complexes the bond to the apical ligand corresponds to *z*. Because this ligand interacts directly with the odd-electron d_{z²} orbital, its hyperfine coupling is large, typically being resolved at *g*₃ in an EPR spectrum (with ¹⁴N, the coupling is ca. 50 MHz for Co(II)³² and ca. one-third larger for Ni(III)).^{33,34} The couplings to in-plane ligands are small and not resolved by EPR, but they can be characterized by ENDOR/ESEEM^{32,35} studies; for ¹⁴N ligands to Co(II) these couplings are over 10-fold less than those to the out-of-plane ligand. The unique (largest) hyperfine tensor component for a ligand to a d_{z²} ion is found to lie roughly along the metal–ligand bond.³⁶

Given the above, one would expect the *g*₃ axis of the **g** tensor of *Dg* Hase to point at the bridging S(Cys533), which forms the apex of the distorted square-pyramid of the nickel ion, and, indeed, such an orientation has been reported for the Ni/Fe center of *DvM* Hase.³¹ If this orientation also occurred for *Dg* Hase, the ¹⁷O bridge would lie in-plane and should have a small hyperfine coupling, as is observed here. However, one would also expect the hyperfine tensor of the ¹⁷O bridge to be collinear with **g**, with the unique (largest) tensor component to lie along the Ni–O bond, and thus normal to *g*₃, whereas our ¹⁷O ENDOR results show that the **g** and hyperfine tensors are not collinear; the unique hyperfine component instead makes an angle of $\theta \approx 45^\circ$ with *g*₃. This noncollinearity suggests that the *Dg* Hase **g** tensor does not have an idealized orientation with *g*₃ pointing at the apical sulfur, which is unlike the situation reported for *DvM* Hase, even though the principal *g* values, and indeed the structures, of the dinuclear centers in these two enzymes are extremely similar.

While the noncollinearity in *Dg* Hase may merely reflect details of the hyperfine interactions in this type of center that are not yet understood, it does open the possibility that the O bridge is not lost in Ni-C, but instead that a reorientation of the *z*-axis upon reduction to Ni-C could be placing the O bridge more nearly orthogonal to *z* (increased θ), thereby decreasing the ¹⁷O hyperfine coupling and hindering detection of the ¹⁷O ENDOR signal in Ni-C.

The most direct argument against this possibility is based on the similarity between the ⁵⁷Fe couplings in Ni-C and Ni-A. Any reorientation in Ni-C of the *z*-axis, namely of the odd-electron, 3d_{z²} orbital, must also modulate the spin-delocalization from Ni to Fe through bridging sulfur and thus would be expected to correspondingly modulate the ⁵⁷Fe couplings. Yet this does not happen. Nonetheless, we examined the issue by performing exact calculations of the predicted 35 GHz ¹⁷O ENDOR spectra for an extreme case of an ¹⁷O bridge whose hyperfine couplings are reduced 10-fold from those we measure for Ni-A.³⁷ These simulations yield unresolved spectra with a rather narrow peak (~ 2 MHz in breadth) centered at the ¹⁷O Larmor frequency ($\nu({}^{17}\text{O}) = 6\text{--}7$ MHz), which should be readily detected, especially in the vicinity of *g*₁–*g*₂, but no such peak is seen for Ni-C during any of the redox cycles we carried out.³⁸

We thus suggest that the results of our redox cycling experiments are indeed best interpreted as indicating that the solvent-derived oxygenic bridge we detect in the *Dg* Hase Ni-A,B dinuclear centers is lost upon reductive activation to Ni-C, with the possible result of creating two additional open sites in the Ni/Fe coordination spheres. This conclusion is strengthened by a recent EXAFS study of *Chv* Hase, which has shown that the loss of a short Ni–O bond is responsible for the decrease

(29) Davidson, G.; Choudhury, S. B.; Gu, Z.; Bose, K.; Roseboom, W.; Albracht, S. P. J.; Maroney, M. J. *Biochemistry* **2000**, *39*, 7468–7479.
 (30) Gu, Z.; Dong, J.; Allan, C. B.; Choudhury, S. B.; Franco, R.; Moura, J. J. G.; Moura, I.; LeGall, J.; Przybyla, A. E.; Rosenboom, W.; Albracht, S. P. J.; Axley, M. J.; Scott, R. A.; Maroney, M. J. *J. Am. Chem. Soc.* **1996**, *118*, 11155–11165.
 (31) Trofanchuk, O.; Stein, M.; Gessner, C.; Lenzian, F.; Higuchi, Y.; Lubitz, W. *JBC, J. Biol. Inorg. Chem.* **2000**, *5*, 36–44.
 (32) Van Doorslaer, S.; Schweiger, A. *J. Phys. Chem. B* **2000**, *104*, 2919–2927.
 (33) Lovecchio, F. V.; Gore, E. S.; Busch, D. H. *J. Am. Chem. Soc.* **1974**, *96*, 3109–3118.
 (34) Lappin, A. G.; Murray, C. K.; Margerum, D. W. *Inorg. Chem.* **1978**, *17*, 1630–1634.
 (35) Wirt, M. D.; Bender, C. J.; Peisach, J. *Inorg. Chem.* **1995**, *34*, 1663–1667.

(36) Less likely, for the in-plane ligands the directions might be orthogonal. This case would not alter the following considerations, so it is set aside for now.
 (37) Representative calculations employed, $\mathbf{A} = [0.5, 0.5, 2.0]$ MHz and $\mathbf{P} = [-0.1, -0.1, 0.2]$. Calculations with a variety of orientations of the tensors were not significantly different. Note that with such parameters, where quadrupole and hyperfine interactions are of comparable value, one cannot use the first-order equations reliably.
 (38) We note that the same type of calculation indicates that one could not reliably hope to detect such a signal at X band; because of the 4-fold lower Larmor frequency the spectrum would come at very low frequency, where sensitivity and baseline considerations would almost certainly preclude detection.

in coordination number (from five to four) that occurs in reductive activation of the Ni-B state of the enzyme to Ni-SI.²⁹

Conclusions

The present employs ¹⁷O ENDOR to demonstrate the presence of an oxygenic (O²⁻ or OH⁻) bridge between Ni and Fe in the Dg Hase Ni-A dimetallic center and to further indicate that this bridge is present in Ni-B. The bridge does not exchange with solvent in the Ni-A state. The ¹⁷O interaction disappears upon reductive activation to the Ni-C state. We propose that the bridge is lost upon activation and re-formed from solvent upon oxidation of Ni-C to Ni-A. Coordination sites exposed upon loss of the bridge may play a central role in the enzyme's

activity. The exact nature of the bridge in Ni-A (μ -oxo, μ -hydroxo, or μ -aquo) remains to be determined and is the subject of ongoing investigation.

Acknowledgment. The authors wish to gratefully acknowledge Mr. Clark Davoust. This work was supported by Fundação para a Ciência e Tecnologia, PRAXIS grants 2/2.1/QUI/3/94 (I.M.), 2/2.1/BIO/05/94 (J.J.G.M.), BPD/16362/98 (C.D.B.), BD/5075/95 (M.C.), and BD/11033/97 (A.P.) and the NIH HL 13531 (B.M.H), and also the NSF (MCB 9904018). M.C. and C.D.B also thank PRAXIS for financial support for travel to the USA.

JA010204V